



In pursuit of anomalies—Analyzing the poleward transport of Atlantic Water with surface drifters

I. Koszalka ^{a,*}, J.H. LaCasce ^b, C. Mauritzen ^c

^a Department of Earth and Planetary Sciences, 328 Olin Hall, 3400 North Charles Street, Johns Hopkins University, Baltimore, Maryland 21218, United States

^b Department of Geosciences, University of Oslo, P.O. Box 1022, Blindern, 0315 Oslo, Norway

^c Center for International Climate and Environmental Research (CICERO), P.O. Box 1129, Blindern, 0318 Oslo, Norway

ARTICLE INFO

Available online 7 August 2012

Keywords:

Drifters
The Nordic Seas
Transit times
Anomaly propagation

ABSTRACT

We examine the trajectories of 168 drifters as a proxy for Atlantic water flowing through the Nordic Seas. The drifters were released at or passed through the Svinøy section, off the west coast of Norway. For comparison, we generate a set of synthetic trajectories using a stochastic model, with a range of diffusivities.

With the both sets, we determine the transit times of both drifters and particles from Svinøy to Arctic gateways: the Barents Sea and Spitsbergen. The mean arrival times to these locations are roughly 200 and 500 days, respectively. This implies ample time for cooling of the surface waters, which increases densities and permits subduction before reaching the Arctic. However a range of transit times is seen; some parcels reach Fram Strait in only 4 months while others are still in the southern Nordic Seas after 2 years.

The results do not support the idea that temperature or salinity anomalies can exist as coherent packets. The drifters passing Svinøy, when treated as a group, quickly spread over large distances, mixing with water in the Norwegian and Lofoten Basins. Thus an anomaly entering the Nordic Seas would quickly be obliterated. However, the velocity of the clusters center of mass is consistent with anomaly propagation speeds inferred previously from hydrographic measurements, suggesting the observed variability is advective in nature.

Published by Elsevier Ltd.

1. Introduction

The Nordic Seas, comprising the Norwegian, Iceland and Greenland Seas (Fig. 1A) is the transition zone for the warm, saline water flowing from the Atlantic to the Arctic Ocean. The Norwegian Atlantic Current (NwAC), the poleward extension of North Atlantic Current, is the primary conduit for this flow, connecting the Atlantic Water to the Barents Sea and the Fram Strait (Fig. 1B). The waters cool as they flow northward, submerging and eventually feeding what becomes the North Atlantic Deep Water (Isachsen et al., 2007; Mauritzen, 1996). Thus variations in the properties and/or volume transport of the Atlantic inflow could impact the ventilation of the Arctic Ocean (e.g., Furevik et al., 2007; Rudels et al., 2004) as well as the oceanographic conditions in the Barents Sea (Skagseth, 2008, and references therein).

An interesting question arises though when one considers the *time scales* involved. Fluid parcels in the main branches of the NwAC can move at speeds exceeding 50 cm/sec. As such, they would traverse the distance between the southern Nordic Seas

and Spitsbergen within 2 months. If this were the case, the period of contact with the atmosphere would be too short to account for the observed cooling of the surface waters (Mauritzen, 1996). Alternately, with a poleward transit time of 2 months, the observed temperature drop between the southern Norwegian Sea and the Fram Strait, 4.2 °C (Blindheim and Østerhus, 2005), would correspond to an average heat loss of ~ 800 W/m². This is about ten times the mean annual heat flux inferred from hydrographic measurements (Isachsen et al., 2007).

It is more likely that the parcels are exiting the cores, and thereby taking a longer time to reach Spitsbergen. This in turn would imply mixing between the cores and the interior waters in the Nordic Seas. Indeed, such a mixing is inherent in previous Lagrangian studies in the region (e.g., Andersson et al., 2011; Koszalka et al., 2009, 2011; Poulain et al., 1996). But none of these studies have actually quantified the fluid transit times from the southern Nordic Seas to the North. We do not know how long a “typical” parcel takes to make the journey.

A related question concerns the fate of temperature and salinity *anomalies* in the Nordic Seas. Hydrographic anomalies are regularly observed in the northern North Atlantic. The most familiar are the “great salinity anomalies” (Belkin, 2004; Belkin et al., 1998; Dickson et al., 1988). These structures are surface-intensified, extending to depths of several hundred meters, and

* Corresponding author. Tel.: +1 410 516 5631.

E-mail address: inga.koszalka@jhu.edu (I. Koszalka).

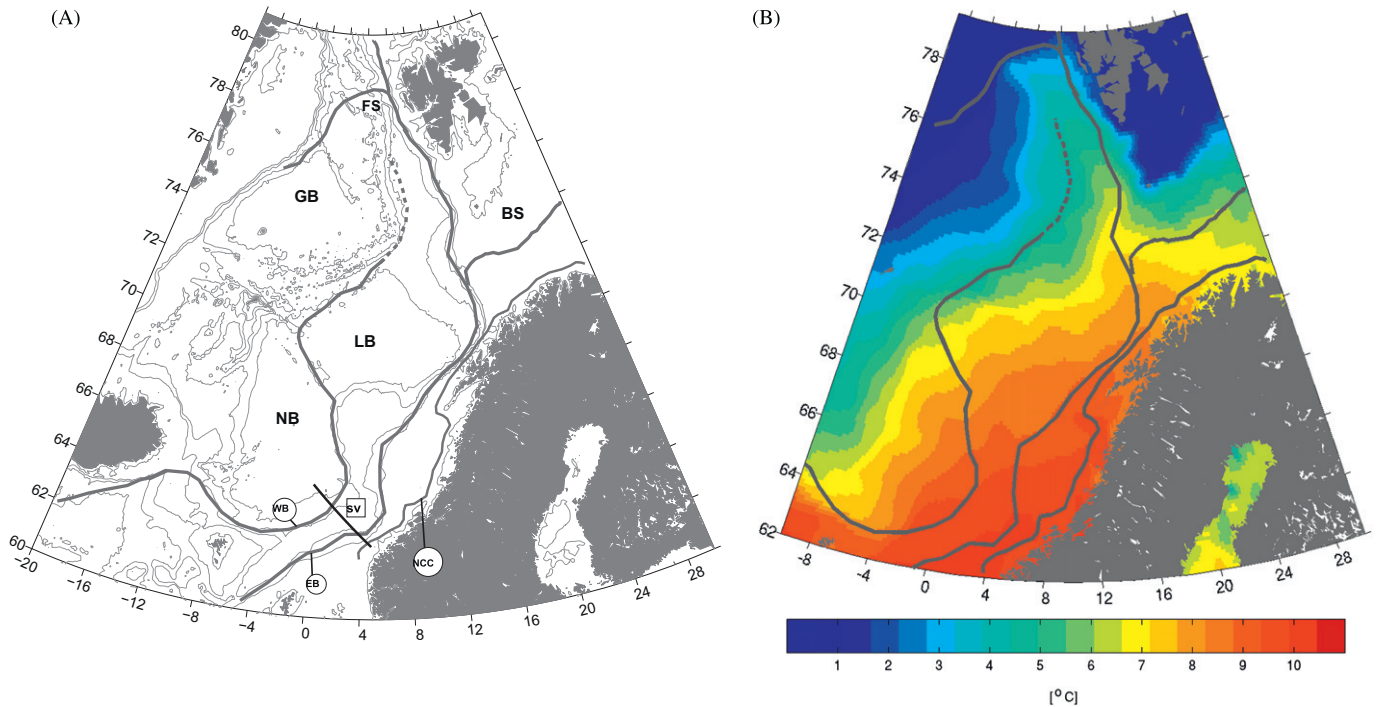


Fig. 1. (A) A schematic of pathways of the Atlantic inflow and main bathymetric features in the Nordic Seas, based on Koszalka et al. (2011). Contour depths of [500,1000, 2000, 2600 and 3000] are shown. Abbreviations: BS=Barents Sea, FS=Fram Strait, GB=Greenland Basin, LB=Lofoten Basin, NB=Norwegian Basin, SV=Svinøy section, VP=Vøring Plateau. The Svinøy section is also marked with a black line. The two branches of Norwegian Atlantic current are the eastern branch (EB) and the western branch (WB); and NCC stands for the Norwegian Coastal Current. (B) The pathways of the Atlantic inflow superimposed on the mean temperature field for the period 2003–2005 (TOPAZ climatology); provided by F. Counillon.

appear to propagate in a coherent way following the mean flow. Sutton and Allen (1997) described a northeast propagation of anomalies generated in the Gulf of Mexico, reaching the Iceland-Shetland Ridge after 12–14 years. Salinity anomalies have also been observed in the Subpolar Gyre, moving with speeds of 3–10 cm/s (Belkin, 2004).

Hydrographic anomalies have been documented in the Nordic Seas since the early 20th century (Helland-Hansen and Nansen, 1909; Jakhelln, 1936). Using time series from the Rockall Channel and Bear Island, Blindheim and Loeng (1981) deduced that there were anomalies propagating northward, with a time lag of 2–3 years. Similarly, Furevik (2001) and Polyakov et al. (2005) suggested that warm anomalies were being advected through the Nordic Seas with speeds of 3–4 cm/s. Holliday (2008) reached a similar conclusion, that anomalies are being advected through the region by the mean flow. However, Sundby and Drinkwater (2007) questioned whether the anomalies are actually advected coherently through the domain. The observed changes, they suggested, could instead stem from variations in the volume flux of the inflow. The latter is correlated with the North Atlantic Oscillation index, that is, the large-scale atmospheric forcing.

Hereafter, we infer the motion of hydrographic anomalies by following the motion of fluid parcels. This can be done with Lagrangian instruments, like floats and drifters (LaCasce, 2008; Lumpkin and Pazos, 2007; Rossby, 2007; Rossby et al., 1983). We examine the trajectories of 148 surface drifters deployed in the southern Norwegian Sea during the POLEWARD project, combined with additional trajectories from the historical archive. We demonstrate that although the center of the mass of a group of water parcels moves poleward at speeds comparable to those reported earlier, the clusters spread over the eastern Nordic Seas in a few months. Thus, it is unlikely that a group of water parcels should remain tightly constrained during the 2000 km, 2-year transit of the Nordic Seas. We find too that similar transit time

distributions can be obtained using a set of synthetic particles generated using a stochastic routine.

2. Data and methods

2.1. Drifter data

For the drifters, we use both the Poleward data and the historical data from the region; both are available under the Global Drifter Program.¹ The instruments are standard Surface Velocity Program (SVP) drifters (Lumpkin and Pazos, 2007). Each drifter consists of a surface buoy, with a transmitter and a temperature sensor, and a subsurface drogue at 15 m depth. The buoys are tracked by the Argos satellite system, yielding positions with 150–1000 m accuracy up to 50 times a day. The temperature sensor is 30 cm below the sea surface and has an accuracy of 0.1 °C. Both the buoy positions and temperature series are quality-checked and interpolated by a kriging technique into 6-h intervals at the Drifter Data Center at AOML. The data spans the period 1990–2010, with ~100,000 drifter days from over 400 drifters. The same data were used previously to estimate the time-mean surface circulation and eddy statistics (Koszalka et al., 2011), and its time variability (Andersson et al., 2011), and are described in detail therein.

2.2. The Svinøy section

To investigate the poleward transit of the Atlantic Water through the Nordic Seas, the Svinøy section is a natural starting point. The main currents bifurcate at the Barents Sea opening,

¹ <http://www.aoml.noaa.gov/phod/dac/gdp.html>.

so we will use this location, and the exit to the Arctic Ocean through the Fram Strait, as end points. The study section is bounded by the Norwegian coast at 62.5°N and encompasses both branches of the Norwegian Atlantic Current (NwAC): the western branch, located over the 2000 m isobath and the eastern branch, 40 km wide and located near the shelfbreak. Both branches are approximately 500 m deep and 30–50 km wide, with average surface speeds of 30 cm/s (LaCasce, 2005; Orvik et al., 2001). The eastern branch is flanked inshore by the fresher Norwegian Coastal Current (NCC). Long-term observations at Svinøy (Orvik and Mork, 1996; Orvik et al., 2001) have been used to study the long-term variability of the Atlantic inflow (e.g., Mork and Blindheim, 2000; Orvik and Skagseth, 2005), allowing the detection of temperature and salinity anomalies (Polyakov et al., 2005). The Svinøy section is also an area with excellent drifter coverage.

We identified 168 drifters that were either deployed at, or passed through, the Svinøy section. This includes 91 drifters released during the POLEWARD experiment in 2007–2008 (Koszalka et al., 2009). Of the remaining 76 drifters that passed through Svinøy, 7 were deployed on the Norwegian continental shelf at 62°N in the 1990s (Saetre, 1999), 10 were advected from the North Atlantic in 2002–2007, while the remaining 58 came from the releases in the Iceland–Faroe Islands area throughout the 1990s (Poulain et al., 1996).

We treat the drifters together as a line of particles released at the Svinøy section simultaneously. Thus, we make the tacit assumption that the mixing properties in the region are stationary in time. Previous studies indicate that while the mean flow exhibits seasonal variations, the eddy diffusivity does not, consistent with this (Andersson et al., 2011). Most of the drifters nevertheless pass Svinøy at different times, and this can affect our interpretation of the motion as a coherent cloud. But many of the drifters in POLEWARD were deployed in pairs and triplets (Koszalka et al., 2009), and we will exploit the information gained from their motion.

2.3. Synthetic drifters

For comparison with the observations, we also generated a set of synthetic drifter trajectories, using a stochastic model. Since the stochastic particles have entirely uncorrelated motion and disperse in a quantifiable manner, they provide a valuable basis for comparison. In addition, the model permits generating many trajectories, thereby increasing the statistical significance.

For this we employed a first-order stochastic model. Similar models have been used previously to simulate the dispersion of surface drifters and of subsurface floats, both in the ocean and in numerical ocean models (e.g., Berloff and McWilliams, 2002; Falco et al., 2000; Griffa et al., 1995; Griffa, 1996). We used the model previously to study dispersion in the Nordic Seas (Koszalka et al., 2009). Higher order models (Berloff and McWilliams, 2002; Veneziani et al., 2004) are an option, but we choose the first-order model for simplicity. Moreover the Lagrangian time scale ($T_L \sim 1$ day) is sufficiently short to regard the accelerations as uncorrelated. The particle positions in the first-order model are given by

$$dx_i = [u_i + U(x,y)] dt, \quad dy_i = [v_i + V(x,y)] dt, \\ du_i = -\frac{1}{T_L} u_i dt + \sqrt{\frac{2}{T_L}} v dw, \quad dv_i = -\frac{1}{T_L} v_i dt + \sqrt{\frac{2}{T_L}} v dw. \quad (1)$$

Here, the subscript i refers to the particle number, (U,V) is the background mean flow and dw is a Wiener noise process. The two free parameters are v , the rms eddy velocity, and T_L , the Lagrangian integral time scale. The eddy motion is assumed isotropic and the

two components of the velocity u and v are independent. The asymptotic value of eddy diffusivity in the model is $\kappa = v^2 T_L$.

For the time-mean velocities, $[U(x,y), V(x,y)]$, we use the estimates of the surface currents in the Nordic Seas obtained from the drifter data using the clustering method (Koszalka et al., 2011). These values were re-sampled on a regular grid $(long, lat) = 0.4^\circ \times 0.2^\circ$. This grid size, corresponding to a length scale of ~ 20 km, is comparable to the widths of the main branches of the NwAC. The means were then linearly interpolated onto the particle's instantaneous positions for advection.

As noted, the integral time, T_L , is roughly 1 day (Andersson et al., 2011). Thus, to quantify the effect of the eddy diffusivity on the transit times, we ran the model with T_L fixed and varied only the rms velocity, v . We will consider the following scenarios:

1. Non-diffusive: $\kappa = 0$.
2. Weakly diffusive: $\kappa = 500 \text{ m}^2 \text{ s}^{-1}$, $v = 0.076 \text{ m/s}$.
3. Average-diffusivity: $\kappa = 1100 \text{ m}^2 \text{ s}^{-1}$, $v = 0.113 \text{ m/s}$.
4. Strongly diffusive: $\kappa = 4000 \text{ m}^2 \text{ s}^{-1}$, $v = 0.215 \text{ m/s}$.

In the first case, the particles are advected only by the mean flow. In the third case, the diffusivity is roughly the same as the average value estimated by Koszalka et al. (2011). Cases 2 and 4 have smaller and larger diffusivities, respectively.

We also ran the model using spatially variable diffusivities (modifying the model appropriately to obey the “well-mixed” criterion of Thompson (1987); see Rodean, 1996; Berloff and McWilliams, 2002). Indeed, the diffusivities in the region estimated from surface drifters are variable (Koszalka et al., 2011). However, the results were not more realistic than those obtained with a constant diffusivity. Thus we chose to focus on the latter, for simplicity.

In each run, ten stochastic particles were deployed at the same position as an actual drifter at Svinøy, yielding 1680 particles. Note that individual particle motion in the stochastic model is uncorrelated, so using the same starting location is not problematic.

The particles were then advected for 2 years with a time step $dt = 0.1$ day. We applied a reflection condition for particles striking the coast or islands, or entering areas not sampled by

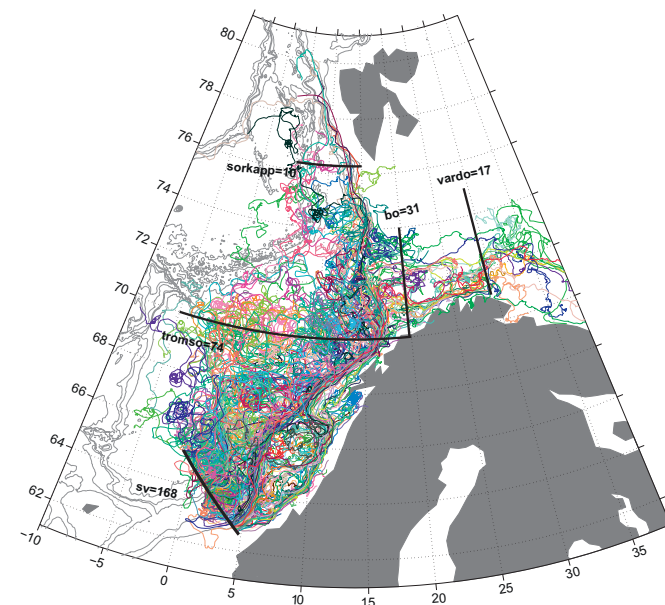


Fig. 2. The trajectories of 168 drifters originating at the Svinøy section. The key sites used to calculate the transit times are also drawn: the Barents Sea Opening (BO), the Vardø section and the Sørkapp section in the Fram Strait. The number of drifters recorded at these sites is also given.

Table 1

Arrivals of drifters to the sections along the pathway of the Atlantic Waters in the Nordic Seas (shown in Fig. 2): Tromsø, Barents Sea Opening (BO), Vardø and Sørkapp. Listed are: geographical coordinates, distance from the Svinøy section (*dist-xy*), yardstick distance along 1000 m-isobath for Tromsø and Sørkapp, and along the 250-m isobath for BO and Vardø (*dist-topo*), the number of drifters (*NoD*) recorded at section, mean transit time from drifters ($\langle T_d \rangle$) in days and mean transit time for the stochastic simulation with $\kappa = 500 \text{ m}^2 \text{ s}^{-1}$ ($\langle T_m \rangle$): 2-year simulation with particle mortality (2y-m), 2-year simulation, no particle mortality (2y), 4-year simulation, no particle mortality (4y) and a 10-year long simulation without the mortality (10y). For the calculation of the distances, the (ETOPO2v2) data set was used, smoothed with a Gaussian filter with a length scale of 10 km.

Section	Coordinates	dist-xy (km)	dist-topo (km)	NoD	$\langle T_d \rangle$	$\langle T_m \rangle$ 2y-m/2y/4y/10y
Tromsø	–5–10°E, 70°N	720	960 ^h = –1000 m	74	109	138/149/161/190
Barents Sea	20°E, 70–74°N	1100	1100 ^h = –250 m	31	181	201/205/224/269
Vardø	29.5°E, 7–75°N	1440	1500 ^h = –250 m	17	261	279/281/325/374
Sørkapp	5–15°E, 76.3°N	1410	1750 ^h = –1000 m	10	326	317/425/493/591

the original drifters. The Barents Sea (30°E) and Fram Strait (77°N) were treated as “absorbing” boundaries, i.e. the particle trajectories were terminated here.

3. Results

3.1. Spreading of the water parcels

The drifter trajectories originating from the Svinøy section are plotted in Fig. 2. The figure also indicates sites where long-time hydrographic- and mooring observations are available. One is the Sørkapp section, near the Fram Strait, where the flow has been monitored since 1978 (76.3°N, 5–15°E, see e.g., Holliday, 2008). The second is the Barents Sea Opening (20°E and 71–74°N) operated since 1997 (Skagseth, 2008) and extended here south to 70°N. We define two additional sites for our analysis: the Tromsø section, along 70°N, and the Vardø section, along the 29.5°E. We use the latter to gauge the transit in the Barents Sea. The geographical coordinates for these sites, distances from the Svinøy section and number of drifters recorded are listed in Table 1.

As seen in the figure, the drifters generally move northward, until they reach $\sim 71^\circ\text{N}$. After that, the trajectories split. One group continues northward toward the Fram Strait while the other turns eastward into the Barents Sea. The inflow to the Barents Sea (72–74°N) is accompanied by several recirculations (as described by Ingvaldsen et al., 2004). Some of the drifters moving toward Fram Strait recirculate westward at 74–77°N, while the rest move into the Arctic Ocean with the West Spitsbergen Current.

Some of the main currents are discernible in the figure. The eastern branch of the NwAC is seen clearly, as is the Norwegian Coastal Current (NCC), south of 68°N. The NwAC and NCC appear as a single branch, south of the Barents Sea inflow at 71.5°N. The pathway of the western branch of the NwAC is, on the other hand, hardly seen. Rather, the trajectories cover the area west of the eastern branch fairly uniformly. Note though that the drifters do not enter the Iceland or Greenland Seas, implying the surface dispersion is affected by the submarine ridges (e.g. Rossby et al., 2009).

The number of active drifters as a function of time since passing Svinøy is shown in Fig. 3. The number of drifters decreases with time as the instruments cease transmission or lose their drogues. The population exhibits approximately an exponential decay, with an e-folding time of 161 days. This is less than half of the mean for the global drifter array (450 days, Lumpkin et al., 2012), suggesting that the Nordic Seas is a particularly hostile environment for drifters. After 1 year, there are only 17 transmitting drifters remaining. Out of 168 drifter losses, 62 can be explained by environmental conditions: there were 45 instances of running aground and 17 buoys were likely

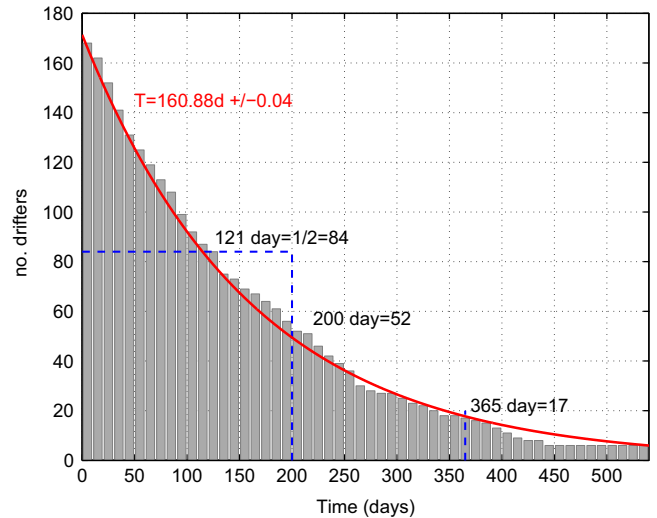


Fig. 3. The histogram of the number of drifters deployed at, or passing by the Svinøy section as a function of time. The red curve shows the exponential decay law fitted to the total number of available drifters, which has a time scale of $\tau = 160.88$ day. (For interpretation of the references to color in this figure caption, the reader is referred to the web version of this article.)

destroyed by ice in the Fram Strait and in the Barents Sea; 7 drifters were classified by the AOML as picked-up by fishermen. The remaining drifter losses are likely due to battery performance and/or the strain tether sensor (“quit events”).²

Drifter mortality complicates evaluating transit times to the various sections. For instance, more drifters reach the Barents Sea Opening (31) than the Sørkapp section (10). But the distance to the latter is larger (~ 900 km vs 1500 km), which increases the possibility for drifter failure. The falling number of drifters also increases the statistical error and biases the transit times to the faster moving buoys.

Fig. 4 shows the distribution of drifters in the Nordic Seas at various times (10, 30, 60, 90, 120 and 200 days) after the departure from the Svinøy section. Error ellipses (defined as the 50%-confidence region for the drifter positions) and the cluster center of mass are also indicated. The Svinøy drifters spread and fill the eastern Nordic Seas within 4 months. While the fastest drifters reach the Barents Sea Opening and the Fram Strait in 2 and 3 months respectively, some remain in the Svinøy region after 200 days.

At 30 days, the mean cluster position is near the eastern branch, following the continental slope. After ~ 100 days, when

² A recent re-evaluation of the drifter quit events suggests that many were undetected pick-ups (Lumpkin et al., 2012). Indeed, nearly all the quit events in the Nordic Seas occurred in the intensively fished Norwegian Economic Zone.

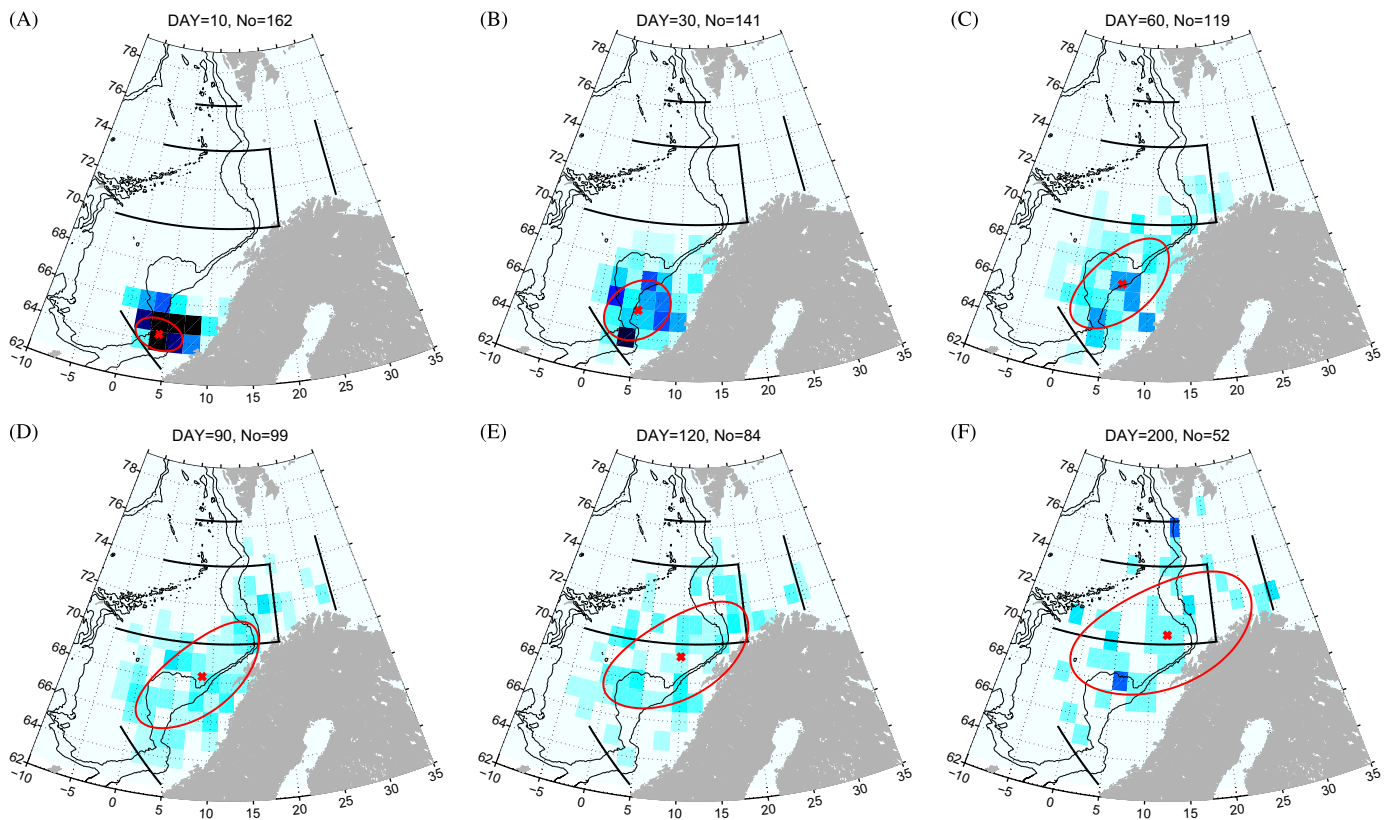


Fig. 4. Distribution of drifters released as a “cluster” at Svinøy in function of time: (A) 10 days, (B) 30 days, (C) 60 days, (D) 90 days, (E) 120 days and (F) 200 days, calculated by gathering the data into geographical bins ($long, lat = 2^\circ \times 1^\circ$) and normalized by the instantaneous number of drifters No (listed in the title). The error ellipses define 50%-confidence region for the drifter position and are drawn with a red line. The positions of the center of mass for the cluster are depicted with a red cross. Superimposed are 1000 m and 2000 m isobaths. (For interpretation of the references to color in this figure caption, the reader is referred to the web version of this article.)

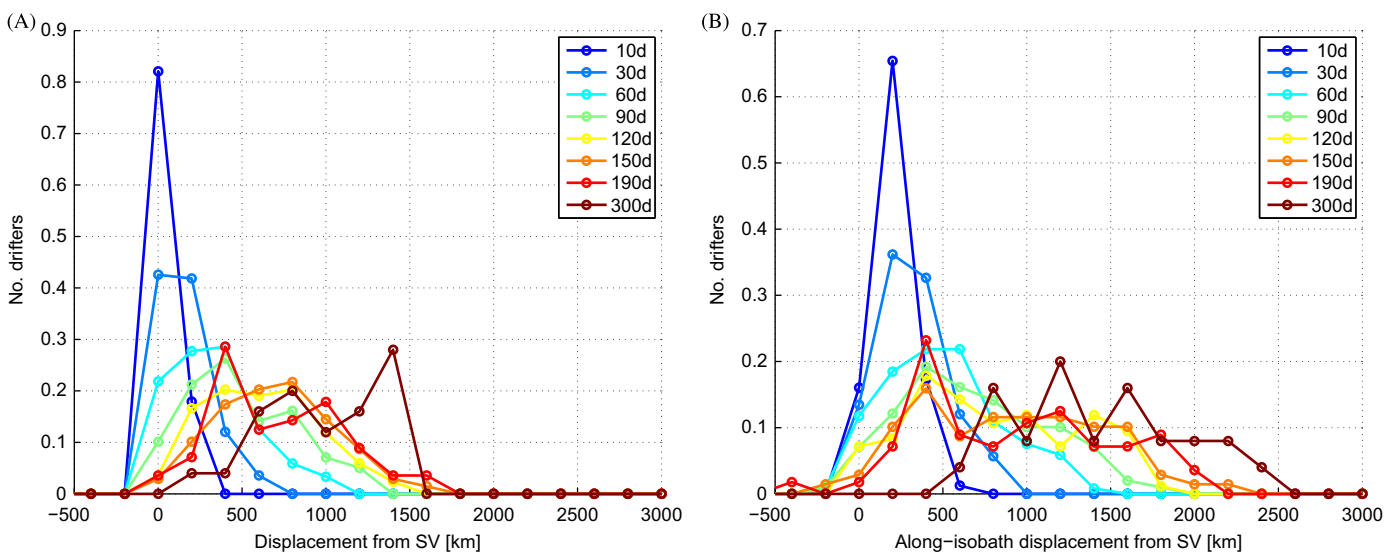


Fig. 5. Left: Snapshots of distributions of absolute distances (left) and along-isobath displacements (right) for drifters originating at the Svinøy section and spreading in the Nordic Seas. Displacements were gathered in 200 km-bins, and normalized by the instantaneous number of available drifters. The origin ($x=0$) corresponds to the particle starting position at the Svinøy section.

passing over the Lofoten Escarpment ($\sim 12^\circ E, 69^\circ N$), the center of mass moves off the slope towards the center of the Lofoten Basin where it resides for next ~ 100 days. Thereafter it moves slowly northward along the eastern part of the Basin approximately 200 km from the coast. During this time, the error ellipses grow, reflecting the cluster spread.

We can quantify drifter spreading by using probability distribution functions (PDFs) of the drifter displacements. For this, we use the total distance from Svinøy, $dist = \sqrt{x_{SV}^2 + y_{SV}^2}$, where $(x_{SV}(t), y_{SV}(t))$ are the zonal and meridional displacements at time t . We use distance (rather than, say, latitude) because the flow is not unidirectional; for example it is mostly

meridional into the Fram Strait, but nearly zonal into the Barents Sea. Using the displacement effectively collapses the 2-D distributions seen in Fig. 4 onto 1-D PDFs. Thus while we lose information about the lateral distribution of the drifters, the PDFs are simpler to visualize the poleward progression of drifters.

The PDFs are shown in Fig. 5A. We calculate these by generating a histogram of the displacements and then normalizing by the number of drifters present at that time (so that the integral of the PDF is one). Thus the procedure compensates for drifter mortality. The PDF initially is a delta-function, because all drifters start on the line at Svinøy. The PDF rapidly broadens, to over 400 km after 10 days. The wings of the PDF (large displacements) correspond to a group of drifters carried in the eastern branch and in the NCC, with velocities exceeding 0.5 m/s. After 4 months the drifters have spread over 1500 km. Interestingly, the spreading is largest between ~90–200 days, when the cluster center of mass barely moves; this occurs as the drifters enter the Lofoten Basin. After 200 days a group of drifters reaches 1500 km distance (corresponding to the locations of Sørkapp and Vardø sections), while some of the buoys are still in the Svinøy region. Again, the fast moving drifters are in the eastern core of the NwAC and the NCC; the slower ones get trapped in the recirculations or in the Lofoten Basin (not shown).

Since the circulation in the Nordic Seas is topographically steered (Isachsen et al., 2003; Koszalka et al., 2009, 2011; Nøst and Isachsen, 2003; Søiland et al., 2008), we also examined the distances along topographic contours. For this, we used the 2-min Gridded Global Relief Data set (ETOPO2v2)³ and applied the method of LaCasce (2000), projecting drifter velocities along and across the depth contours. The projection requires smoothing the bathymetry, and for this we used a Gaussian filter with a length scale of 10 km (comparable to the internal radius of deformation in the Nordic Seas). This value maximizes the anisotropy between the along- and across-isobath dispersion (LaCasce, 2000). The displacements relative to topography are then obtained by integrating the projected velocities.

The PDFs relative to the topography are shown in Fig. 5B. These agree well with those calculated with distance, except at the larger separations where the along-isobath PDFs exhibit larger displacements. This is due in part to the curvature of the isobaths; the distance along an isobath is greater than the absolute distance to the starting point if the isobath is not straight. However, drifters recirculating (in the Lofoten Basin and near Fram Strait) also cause the along-isobath distance to increase (as we do not “reset” the distance on closed circuits). The largest along-isobath distances are roughly 2500 km, as opposed to 1500 km in absolute distance.

3.2. Synthetic drifters

The trajectories of the stochastic particles with the different diffusivities are shown in Fig. 6. In the following, we will focus on the region south of 73°N. The actual drifter trajectories are also shown, for comparison (top panel).

The trajectories simulated without diffusion (middle left panel) trace out the mean currents in the Nordic Seas. Both branches of the NwAC and the NCC are seen, as is the flow connecting the western and eastern branches along the Vøring Plateau. Several permanent recirculations with ~100 km scales are also evident, and these slow the poleward transit. In addition,

there are three distinct streams entering the Barents Sea: two attributable to NwAC and one due to the NCC (e.g., Skagseth, 2008).

Adding diffusion causes the particles to exit the mean currents. Even with the smallest diffusivity ($\kappa = 500 \text{ m}^2 \text{ s}^{-1}$, middle right panel) the particles spread over the Vøring Plateau and enter the Lofoten Basin. Using the average value of diffusivity ($\kappa = 1100 \text{ m}^2 \text{ s}^{-1}$, bottom left panel) captures the spreading of real drifters, but also overestimates the exit of particles from the eastern branch and the NCC. The case with the high diffusivity ($\kappa = 4000 \text{ m}^2 \text{ s}^{-1}$, bottom right panel) displays unrealistically vigorous spreading.

Fig. 7 shows PDFs of the particle displacements from Svinøy for the different model experiments and for the drifter data, at four times (30, 60, 120, 200 days). As noted, the total number of drifters decays in time. For consistency, we imposed the same exponential decay law on the stochastic particles. Specifically, at each time we terminated a number of particles to duplicate the observed decay. The indices of the particles were taken randomly from the available set.

Notably, even the non-diffusive case shows a substantial spreading in distances, reflecting the different advection speeds in the mean currents. After about 2 months, the non-diffusive case exhibits two peaks. One corresponds to a group of particles following the NwAC and NCC. The other corresponds to slower-moving particles in the west and to those which get trapped in the recirculations (Fig. 6, middle right panel).

Diffusion causes the particles to exit the mean currents and spread, and the PDFs are accordingly broader. Interestingly, *all* the diffusive model runs yield similar PDFs, irrespective of the exact value of κ . Initially, the diffusive cases underestimate the tail of the PDF, as some of the actual drifters travel further. This is because the stochastic particles too readily exit the main currents (compare with Fig. 6). After 3 months though (Fig. 8D), the diffusive cases agree with the drifter PDF quite well. Using the Kolmogoroff–Smirnov test (Press et al., 1992), we find that the PDFs at the late time are not significantly different from one another, or from PDF for the drifters.

Thus the stochastic particles essentially capture the dispersion of the actual drifters. The reason that the PDFs are so weakly affected by the diffusivity is because, with the exception of the recirculations, the flow is poleward over essentially the whole region. Thus the diffusive motion shifts particles laterally, sampling the entire range of poleward flow. Because the distance PDF is one-dimensional, we have effectively integrated over lateral inhomogeneities. Only when the diffusivity is zero do the stochastic PDFs differ, as then the particles are confined to mean currents.

Of the 4 stochastic runs, the distribution of trajectories for the $\kappa = 500 \text{ m}^2 \text{ s}^{-1}$ run most closely resembles that from the drifters (Fig. 6). On a more quantitative level, the $\kappa = 500 \text{ m}^2 \text{ s}^{-1}$ run yields bin-averaged particle densities and residence times closest to those from the observations. Thus we will use that run for the statistical comparisons which follow.

3.3. Transit speeds and times

Now we consider the transit speeds and times for drifters originating at Svinøy. We will focus on the transits to the Tromsø section (at 70°N), to the Fram Strait (Sørkapp section) and into and through the Barents Sea (Barents Sea Opening and Vardø sections), see Fig. 2. The distances from the Svinøy section, both absolute and with respect to the topography, are listed in Table 1.

A general picture can be obtained by considering the motion of the cluster center (Fig. 4). We plot this as a cluster velocity,

³ U.S. Department of Commerce, National Oceanic and Atmospheric Administration, National Geophysical Data Center, 2006. <http://www.ngdc.noaa.gov/mgg/fliers/06magg01.html>.

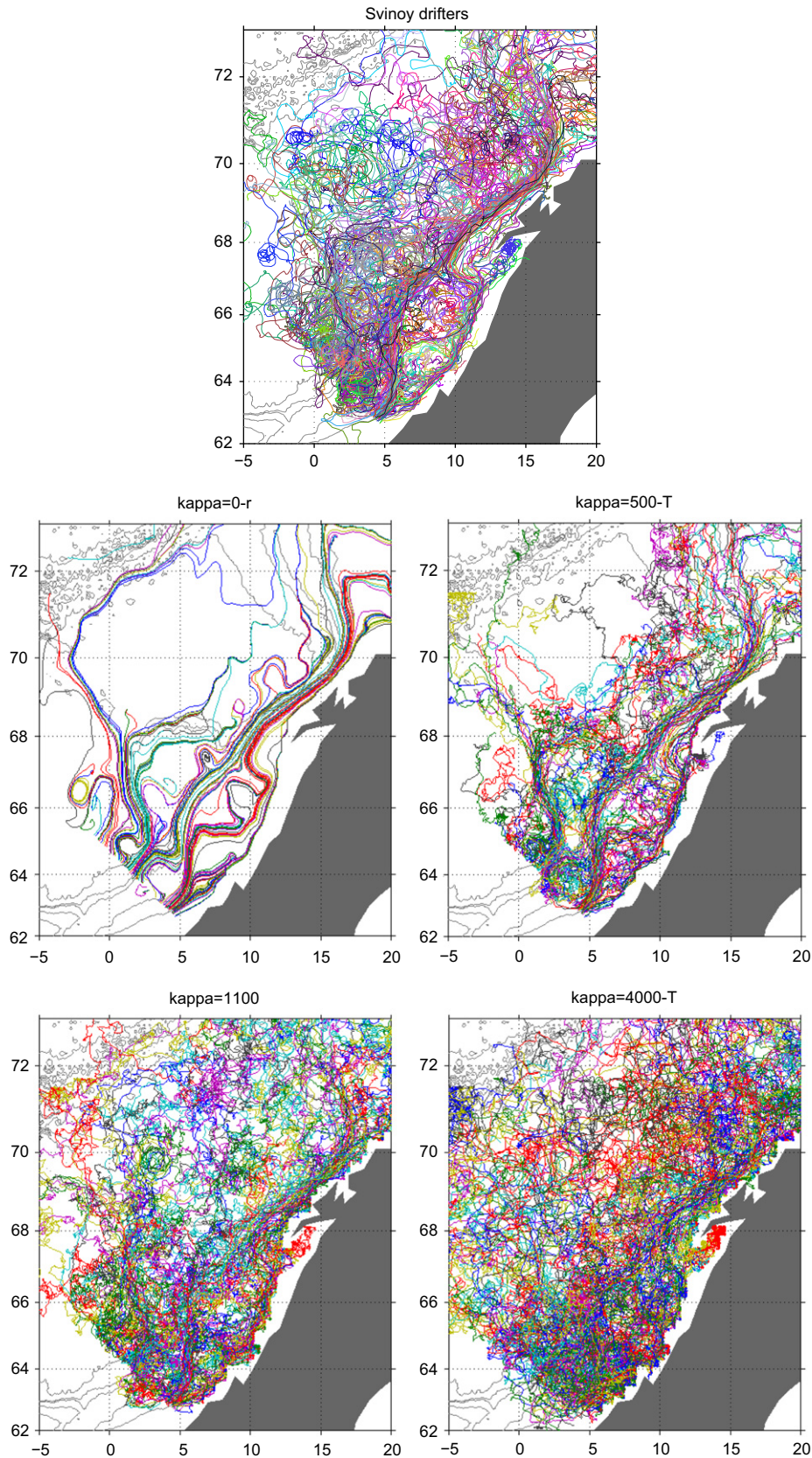


Fig. 6. Trajectories of the 168 Svinøy drifters (top) and trajectories of synthetic drifters from the stochastic model with different diffusivity levels (see Section 2.3): $\kappa = 0 \text{ m}^2 \text{ s}^{-1}$ (case 1, no diffusivity), $\kappa = 500 \text{ m}^2 \text{ s}^{-1}$ (case 2, low diffusivity), $\kappa = 1100 \text{ m}^2 \text{ s}^{-1}$ case 3, (mean diffusivity) and $\kappa = 4000 \text{ m}^2 \text{ s}^{-1}$ (case 4, high diffusivity). For clarity, only one of the ten 168-particle sets from each stochastic run is plotted.

u_p , in Fig. 8. The velocity is $\approx 4 \text{ cm/s}$. However, the speed is greater ($\sim 8\text{--}10 \text{ cm/s}$) during the first ~ 80 days, when the

center of mass follows the continental slope. After that it drops rapidly, as the drifters deviate into the Lofoten Basin (compare

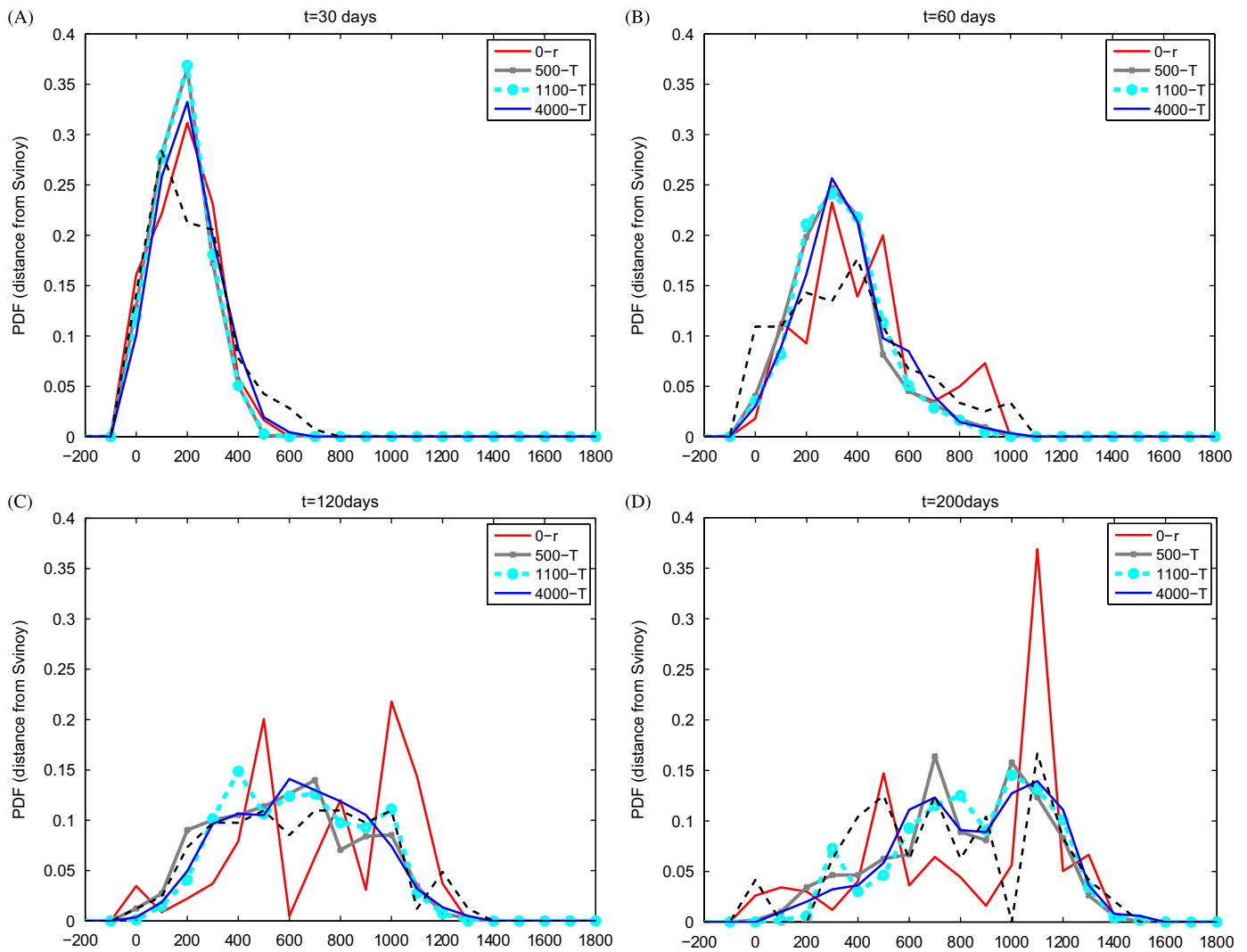


Fig. 7. Snapshots of distributions of absolute displacements of stochastic particles for different values of diffusivity (see Section 2.3): $\kappa = 0 \text{ m}^2 \text{ s}^{-1}$ (case 1, no diffusivity), $\kappa = 500 \text{ m}^2 \text{ s}^{-1}$ (case 2, low diffusivity), $\kappa = 1100 \text{ m}^2 \text{ s}^{-1}$ case 3, (mean diffusivity) and $\kappa = 4000 \text{ m}^2 \text{ s}^{-1}$ (case 4, high diffusivity). The corresponding drifter distributions are depicted with black dashed line. The origin ($X = 0$) corresponds to the particle position at the Svinøy section. (A) $t = 30$ days, (B) $t = 60$ days, (C) $t = 120$ days and (D) $t = 200$ days.

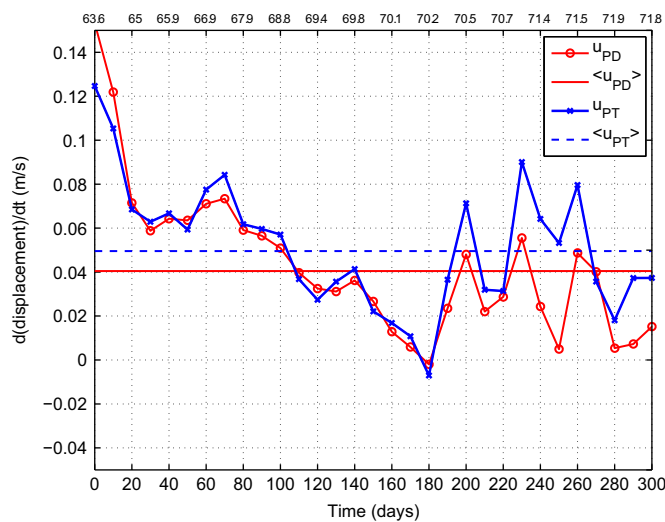


Fig. 8. The mean propagation velocity (the velocity of the center of mass of the cluster of drifters originating at the Svinøy section) in function of time, calculated with respect to the absolute displacement (u_{PD}) and along-isobath displacement (u_{PT}). The top axis shows the meridional position ($^{\circ}\text{N}$ latitude) of the center of the mass.

with Fig. 4, bottom panels). After a 100-day period of a very slow propagation along the eastern Lofoten Basin, the cluster center resumes the poleward journey with $u_p \approx 4\text{--}5 \text{ cm/s}$. One can also calculate the mean along-isobath speed. This is slightly larger ($\approx 5 \text{ cm/s}$), as the distances along the curved bathymetry are larger (compare with Fig. 5). But the picture is largely the same.

The PDFs of the transit times, T , for the actual drifters are shown in the upper panel of Fig. 9. The distributions are fairly noisy, due to the relatively small numbers of drifters. Due to drifter mortality, the northern-most distributions are the noisiest. Nevertheless, several aspects are apparent. The majority of the particles reach the Tromsø section after ~ 100 days; the fastest and slowest arrivals at this section are 2 months and 1 year respectively. On the other hand, only 10 drifters reach the Sørkapp section (absolute distance of 1410 km and along-isobath distance of 1750 km) and their arrival times vary from 3 months to 2.5-years. The modal transit time to the Barents Sea Opening (distance $\approx 1100 \text{ km}$) is about 4 months, but arrivals as late as 2 years are also seen. The transit times to the Vardø section in the eastern Barents Sea (distance $\approx 1500 \text{ km}$) span the range between 3 months and 2 years.

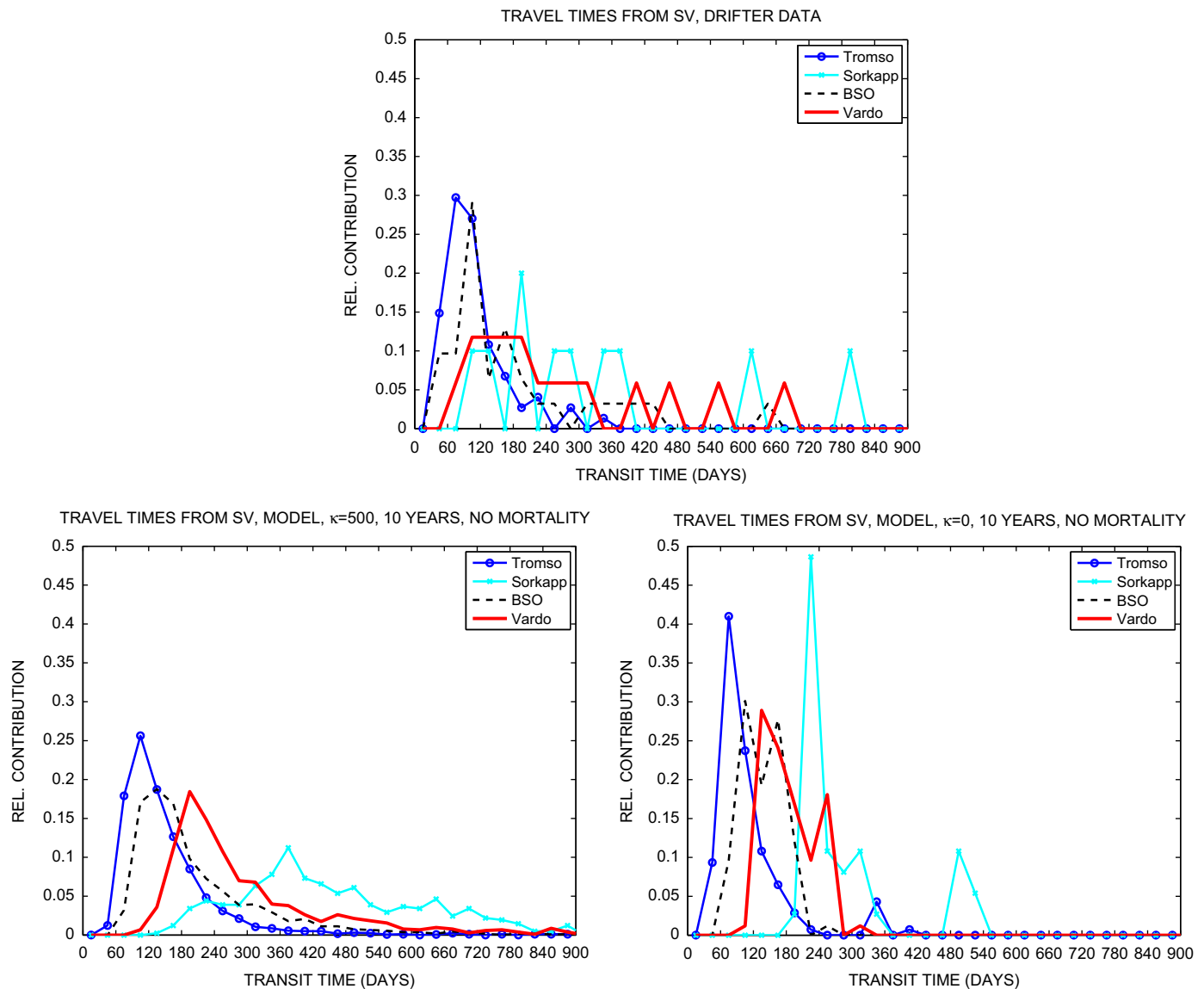


Fig. 9. Upper panel: transit times for the surface drifters released at or advected through the Svinøy section: the Tromsø section (dark blue), the Fram Strait (Sørkapp section, light blue), to the Barents Sea Opening (black line) and to the Vardø section (red line). The corresponding PDFs for the stochastic model with $\kappa = 500 \text{ m}^2/\text{s}$ (lower left) and with $\kappa = 0$ (lower right). (For interpretation of the references to color in this figure caption, the reader is referred to the web version of this article.)

From the distributions, the mean transit times $\langle T \rangle$ can be calculated. These are: 109 days (Tromsø), 181 days (Barents Sea Opening), 261 days (Vardø) and 326 days (Sørkapp). However, as the PDFs have long wings, the mean values do not capture the range of possible values.

As noted, the transit times are potentially biased toward faster arrivals due to drifter mortality. Thus we also calculated transit time PDFs for the stochastic particles, without the imposed mortality. For this we used a 10-year simulation with $\kappa = 500 \text{ m}^2 \text{ s}^{-1}$ and with 1680 particles released at the deployment sites of original 168 drifters at Svinøy. The transit time PDFs are shown in the lower left panel of Fig. 9.

The PDFs are very similar to those from the drifters. But they are also smoother, due to the larger number of particles. Like the drifter PDFs, the peaks shift toward longer times and the wings expand. Interestingly, the wings of the stochastic PDFs are similar to those for the drifters, indicating that the last arrival times are similar. However, the peaks occur at larger times than with the drifters, with the result that the mean transit times are also longer. The means are 161 days (Tromsø), 224 days (Barents Sea Opening), 325 days (Vardø) and 493 days (Sørkapp) for 4-year

trajectories. These are 25–50% longer than corresponding times for the drifters respectively.

There are evidently two reasons why the stochastic transit times are longer. The first is that the initial arrival times are longer with the stochastic model. For example, the probability for arriving at Tromsø after 60 days is roughly 3 times larger for the drifters. The difference is related to the mean flows, which are the fastest means to travel between the sections. As noted, the stochastic particles exit too readily from the mean currents, as the velocity of the stochastic particles is perturbed equally, regardless of whether the particles are in the mean current or not. Had the particles adhered more to the mean currents, the first arrival times would be shorter.

To see this, consider the PDFs obtained with the zero diffusivity model, shown in the lower right panel of Fig. 9. In this case, the model was run for 2 years, which is long enough for many of the particles traversing the domain. While similar to the $\kappa = 500 \text{ m}^2/\text{sec}$ PDFs qualitatively, the peaks are shifted toward shorter times and the probability of short transit times is greater. The mean times—110 days (Tromsø), 136 days (Barents Sea Opening), 187 days (Vardø) and 291 days

(Sørkapp)—are shorter than for both the $\kappa = 500 \text{ m}^2/\text{sec}$ run and the actual drifters. This implies that the actual drifters adhere more to the mean currents than in the weak diffusivity case.

There has been significant interest recently in the suppression of mixing by mean flows (Ferrari and Nikurashin, 2010 and references therein). The mean flow modifies the potential vorticity gradient in its vicinity, and this affects the propagation speed of eddies. Ferrari and Nikurashin (2010) propose a factor by which the diffusivity is decreased near mean flows. We tested this in the present stochastic model and found that it increased the adherence to the mean flows. So, we suspect, it is possible to optimize the model to match the observed transit PDFs.

However, there is a second reason for the difference in mean transit times, related to the lifespan of the drifters. As shown in Table 1, the difference between the stochastic and drifter means depends on the length of the model integration. So, for instance, the mean time to Tromsø for a 2-year simulation with $\kappa = 500 \text{ m}^2/\text{sec}$ is 149 days while that for a 10-year simulation is 190 days. Furthermore, the mean time for a 2-year run with particle mortality imposed is only 138 days.

The reason the longer runs have longer mean times is that particles trapped in various regions of the Nordic Seas weigh more heavily on the averages. Indeed, a non-negligible fraction of the particles are still south of Tromsø after 4 years. Thus the drifters, which have an e-folding time of 160 days, have shorter apparent transit times because the trapped drifters simply die out. Had they survived, the mean transit times would have been longer.

In addition, we tested the sensitivity to the particles initial starting position. For this, we ran an additional set with 2930 particles released uniformly along the line at Svinøy. The PDFs were not significantly different (as measured by the Kolmogorov–Smirnov test) to those with the (inhomogeneous) initial deployment. Thus the exact initial position is not important for the transit times.

Furthermore, we considered the time variability of the transit time statistics. Only the Tromsø and Barents Sea sections have sufficient numbers of drifter arrivals to do this, and the arrivals at these sections are distributed almost equally between the seasons: 33 of the drifters that arrived at the Tromsø section originated at Svinøy during summer months (May–October) and 41 during winter (November–April). For Barents Sea these numbers are 15 and 16 correspondingly. The distributions of arrival times are however almost identical between drifters released during the different seasons for the two sections (not shown), in spite of the fact that the mean flow at Svinøy is 20% stronger during winter (Andersson et al., 2011; Orvik et al., 2001). In addition, there are no discernible differences in the travel times to these sections between the two decades, 1990s and 2000s (33/38 drifters for Tromsø and 17/14 for the Barents Sea).

Previously, the inflow into the Nordic Seas has been related to the NAO index (Mork and Blindheim, 2000). But it turns out that 152 of 168 drifters were deployed at/passed through (Svinøy) during the positive NAO years, and 102 of them were deployed during the phase when the value of the index was within a narrow range ($1-1.5$)⁴. So the present data set does not allow us to study the dependence of the travel time statistics on NAO.

4. Coherent hydrographic anomalies

The present results have implications for the translation of hydrographic anomalies through the region. As we have seen, a

tagged region of fluid will disperse. This is illustrated in Fig. 10, which shows the center of mass and the variance ellipses for the cluster at 10, 30, 60, 90, 120, 180 and 200 days after leaving Svinøy. The drifters start as a coherent line, but spread over 1500 km in only 120 days, filling the eastern Nordic Seas. The ellipses are superimposed over the mean surface temperature contours from 2003, when a warm anomaly was observed at Svinøy (e.g., Polyakov et al., 2005) (most of the drifters were deployed four years later, but we take their motion to be representative). While the drifters originate in the warm waters to the south, the temperature signal weakens as the drifters spread out.

Of course, the ellipses in Fig. 10s derive from drifters deployed at different times—as such, they may not represent the evolution of a tagged region of water. However, the variance of a cloud of tracer is proportional to the mean square separation of all particle pairs in the cloud (e.g. LaCasce, 2008). Koszalka et al. (2009) studied the evolution of pairs deployed together, among the drifters examined here. They found that the mean square pair separation at 30 days was approximately 200^2 km^2 . The radius of the 30-day ellipse in Fig. 10 is also about 200 km. Koszalka et al. (2009) also showed that the pair velocities are correlated only for separations less than 100 km; at larger scales the pair motion is essentially random. So when the ellipses are of the same scale—at roughly 10 days—the fluid motion in the ellipse is similarly random. Thus the variance ellipses in Fig. 10 are entirely consistent with the inferences made for pairs of drifters actually deployed together.

Thus a hydrographic anomaly entering the southern Norwegian seas should disperse as illustrated in the figure. To the extent that the surface velocities are geostrophic (a reasonable assumption at these latitudes), the surface flow is to a first approximation horizontally non-divergent. So such an enormous spreading as seen in Fig. 10 necessarily involves lateral mixing with adjacent waters. As such, a coherent anomaly at Svinøy will rapidly lose its anomalous characteristics, as suggested in the figure.

As a further check, we calculated the temperature difference between the drifter pairs studied by Koszalka et al. (2009). This is shown in Fig. 11B. If the anomaly was to maintain its temperature signature, one would expect the temperature difference on drifters released together to remain constant. Instead, the temperature difference grows as the square root of time; after three weeks, it is approximately $0.5 \text{ }^\circ\text{C}$. The latter is a typical amplitude of an temperature anomaly (e.g., Polyakov et al., 2005). Thus a temperature anomaly should lose its signature over this time. After 3 months (the time the fastest water parcels reach the Sørkapp section) the difference is 1° , and after 1.5 year (the mean travel time for the cluster) it is 2°C , half of the mean temperature change observed over this distance (Blindheim and Østerhus, 2005).

Nevertheless, the mean velocities inferred from the center of mass of the particles are in line with the propagation speeds inferred for the anomalies (e.g. Furevik, 2001; Polyakov et al., 2005). This suggests the latter signals are probably advective in nature. But the question about the coherence remains. In contrast to our expanding ellipses of particles, the Great Salinity Anomalies in the North Atlantic maintain their temporal spread (and hence their spatial extent) over many thousands of kilometers (Belkin et al., 1998; Dickson et al., 1988). We question how such an anomaly would maintain its shape over such distances. Similar points have been made by Wadley and Bigg (2006) and Sundby and Drinkwater (2007).

How quickly do the northward-flowing waters cool? To check this, we used the temperature data from drifters. Fig. 11A shows the mean temperature from the drifters originating at Svinøy as a function of distance from the Svinøy section, calculated in

⁴ The values of NAO index were retrieved from “NAO/NAM Climate Indices”. CGD’s Climate Analysis Section (National Center for Atmospheric Research), <http://www.cgd.ucar.edu/cas/jhurrell/indices.html>, 10 October 2011.

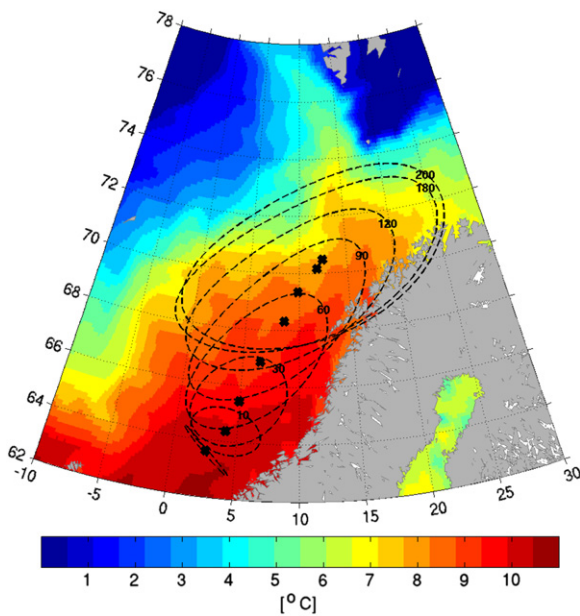


Fig. 10. The variance ellipses for a cluster of drifters originating at Svinøy (crosses) at 10, 30, 60, 90, 120, 180 and 200 days superimposed on the mean surface temperature field from the TOPAZ Reanalysis for 2003—the year of passage of a warm anomaly at the Svinøy section (e.g., Polyakov et al., 2005).

200 km-bins. The latter ensures that there is enough data from different seasons to average out the seasonal cycle. The mean temperatures from drifters passing different sections agree well with hydrographic observations (see Blindheim and Østerhus, 2005, their Figs. 6 and 7), recording $\sim 8.5^\circ\text{C}$ at the Svinøy section, $\sim 7^\circ\text{C}$ at the Tromsø section (extension of the Gimsøy section) and $\sim 4.5^\circ\text{C}$ at the Sørkapp. The temperature drop $\Delta T = 4^\circ\text{C}$ over the distance Svinøy–Sørkapp corresponds to the cooling of $0.0028^\circ\text{C km}^{-1}$. By a simple scaling argument, neglecting the vertical motions and small-scale diffusion processes, the change of the heat content corresponding to this cooling $\Delta H = \rho c_p \Delta T D$, where the density of the sea water is $\rho = 1028 \text{ kg m}^{-3}$, the specific heat $c_p = 3850 \text{ J kg}^{-1} \text{ C}^{-1}$, and the annual mean mixed layer depth in the eastern Nordic Seas $D \approx 250 \text{ m}$ (Nilsen and Falck, 2006), gives $\Delta H/\Delta t \approx 90 \text{ W/m}^2$, taking a representative value of $\Delta t = 500$ days. This agrees well with the value of the heat loss to the atmosphere estimated from the climatology (Isachsen et al., 2007).

5. Summary and discussion

We examined the passage of water parcels from the Svinøy section in the southern Nordic Seas to the Fram Strait and Barents Sea openings. As a proxy for the parcel motion, we used the trajectories of 168 surface drifters, either deployed at or passing through Svinøy at various times. We supplemented that data with synthetic trajectories from a stochastic model, with various diffusivities.

The study was motivated by the question of how long it takes for a parcel to traverse the Nordic Seas. If the flow was confined to the two main cores of the Norwegian Atlantic Current, with maximum velocities over 60 cm/sec, it would only take a matter of months for the journey. As a result, the surface waters would have insufficient contact with the atmosphere to account for the observed cooling (Mauritzen, 1996).

The present results demonstrate that there is in fact a large range of arrival times, as the fluid parcels mix in the regions adjacent to the main cores of the current. While some drifters reach the Fram Strait after only 120 days, others are still lingering at Svinøy at that time.

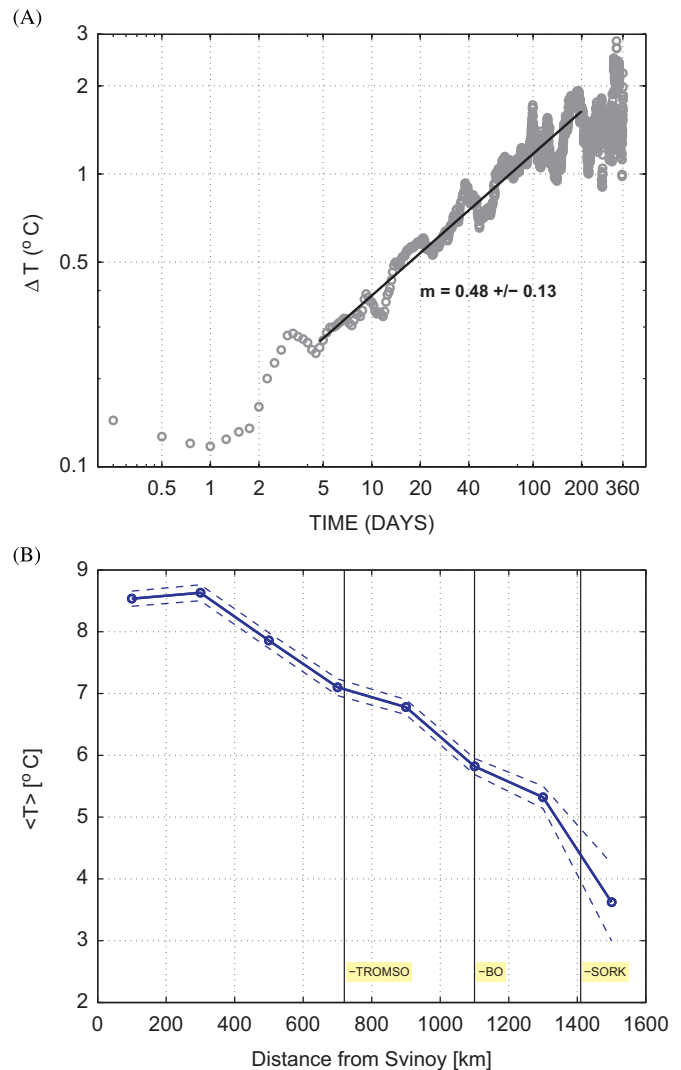


Fig. 11. (A) The temperature difference for pairs of drifters released together in function of time. (B) The mean temperature of the cluster of drifters released at Svinøy in function of distance from the release site calculated in 200 km-bins. Dashed lines represent standard error for the mean, $std/\sqrt{N^*}$, where the number of independent drifter observations is $N^* = N dt/(2T_L)$, N being the number of drifter observations in the bin.

So it makes sense to answer the transit time statistically, in terms of PDFs of arrival times, e.g. at northern Norway or at the Sørkapp section. The PDFs for the drifter data are noisy, due to drifter mortality. But the PDFs from the stochastic data are close enough to the observed distributions to be used for comparisons. We deduce the mean arrival time to the entrance to the Barents Sea is over 200 days, and to the Fram Strait is on the order of 500 days.

Treating the cluster as group, we can calculate the velocity of its center of mass, as shown in Fig. 8. Despite that the drifters essentially fill the eastern Nordic Seas, there is a positive northward drift. Thus the warm “slab” of water in the east is really moving northward with a mean velocity of 4–5 cm/sec. We can compare this to an estimate based on the volume of the inflow (e.g. Mauritzen, 1996). Treating the inflow as a slab with fixed dimensions, the estimated time for the transit to the Sørkapp section (where the total and along-isobath distance from Svinøy is $\sim 1400 \text{ km}$ and 1750 km) is:

$$T = \frac{\text{Volume}}{\text{Transport}} = \frac{400,000 \text{ m} \times 500 \text{ m} \times 1400,000(1750,000) \text{ m}}{8 \times 10^6 \text{ m}^3 \text{ s}^{-1} \times 24 \times 3600} \approx 400(500) \text{ days}, \quad (2)$$

with a corresponding velocity of:

$$u = \frac{1400,000(1750,000) \text{ m}}{T \times 24 \times 3600 \text{ s}} \approx 4(5) \text{ cm/s.} \quad (3)$$

Thus while the “slab” idealization contrasts with the observed structure of the mean currents, it is more representative of the mean motion. This again is because of the extensive mixing between the mean cores.

This mean velocity is not constant. It is greatest in the south, before the drifters reach the Lofoten Basin. There, the drifters pause on their journey. This is seen even when advecting particles without mixing; the particles recirculate in the gyre. The mean velocity drops nearly to zero at this point, before reaching values of 4 cm/sec again to the north. Thus the Lofoten Basin prolongs the contact between the atmosphere and the surface waters, facilitating their cooling (Isachsen et al., 2007; Rossby et al., 2009).

The results have implications for the translation of hydrographic anomalies through the region. A tagged region of fluid will disperse over the entire eastern Nordic Seas and lose its temperature signal in a matter of months. Still, the mean velocities inferred from the center of mass of the particles are in line with the propagation speeds inferred for the anomalies (e.g., Furevik, 2001; Polyakov et al., 2005). This suggests that the latter signals are probably advective in nature. But the question about the coherence remains. It has been suggested that the Great Salinity Anomalies in the North Atlantic maintain their spatial extent over thousands of kilometers (Belkin et al., 1998; Dickson et al., 1988). We wonder how such an anomaly would maintain its structure over such distances. A similar point was made by Wadley and Bigg (2006), who simulated tracer transport in the northern North Atlantic.

As noted, Sundby and Drinkwater (2007) proposed the inter-annual temperature and salinity anomalies could be caused by varying the volume flux into and out of the Arctic Basin, and that such flux variations are correlated with the NAO index. Flatau et al. (2003) suggest that the inflow to the Nordic Seas is correlated with the NAO, and Mork and Blindheim (2000) has shown that the geostrophic volume flux at Svinøy is also correlated with the NAO. Of course the present results, which apply at the surface, cannot be used to diagnose volumetric changes.

Lastly, we note that the first-order model with a constant diffusivity yields reasonable estimates for transit time and displacement statistics. However, the stochastic model is deficient in that particles too readily exit the mean cores. This in turn increases the first arrival times at the northern latitudes. Indeed, some of the drifters actually do take the direct route to Spitzbergen, in the NwAC. To capture this behavior will require using a parametrization like that proposed recently by Ferrari and Nikurashin (2010), in which the diffusivity is suppressed in the mean flows. Finding the “optimal” stochastic model to capture dispersion in the Nordic Seas, would be an excellent follow-up to the present study.

Acknowledgments

The three authors would like to acknowledge Professor Tom Rossby for his continued inspiration throughout the years. Tom has been an important part of the “Lagrangian” community and a good friend. We’ve enjoyed our many interactions with him. We gratefully acknowledge Kjell Arild Orvik and Maria Andersson, our partners in the POLEWARD project. Two anonymous reviewers offered helpful advice on the first draft. The work was funded by the Norwegian Research Council under the Norklima program (grant number 178559/S30). Details can be found on <http://www.iaaos.no/>.

References

- Andersson, M., LaCasce, J., Koszalka, I., Orvik, K., Mauritzen, C., 2011. Variability of the Norwegian Atlantic Current and associated eddy field from surface drifters. *J. Geophys. Res.* 116, C08032.
- Belkin, I.M., 2004. Propagation of the “Great Salinity Anomaly” of the 1990s around the northern North Atlantic. *Geophys. Res. Lett.* 31, L08306.
- Belkin, I.M., Levitus, S., Antonov, J., Malmberg, S.-A., 1998. “Great Salinity Anomalies” in the North Atlantic. *Prog. Oceanogr.* 41 (1), 1–68.
- Berloff, P.S., McWilliams, J.C., 2002. Material transport in oceanic gyres. Part II: hierarchy of stochastic models. *J. Phys. Ocean.* 32, 797–827.
- Blindheim, J., Loeng, H., 1981. On the variability of Atlantic influence in the Norwegian and Barents Seas. *FiskDir. Skr. Ser. HavUnders.* 17, 161–189.
- Blindheim, J., Østerhus, S., 2005. The Nordic Seas, main oceanographic features. In: Drange, H., Dokken, T., Furevik, T., Gerdes, R., Berger, W. (Eds.), *The Nordic Seas—integrated perspective: oceanography, climatology, biogeochemistry, and modelling* (Geophysical Monograph 158), American Geophysical Union, pp. 11–38.
- Dickson, R.R., Meincke, J., Malmberg, S.-A., Lee, A.J., 1988. The Great Salinity Anomaly in the northern North Atlantic 1968–1982. *Prog. Oceanogr.* 20, 103–151.
- Falco, P., Griffa, A., Poulain, P.-M., Zambianchi, E., 2000. Transport properties in the Adriatic Sea as deduced from drifter data. *J. Phys. Ocean.* 30, 2055–2071.
- Ferrari, R., Nikurashin, M., 2010. Suppression of eddy mixing across jets in the Southern Ocean. *J. Phys. Ocean.* 40, 1501–1519.
- Flatau, M.K., alley, L., Niiler, P., 2003. The North Atlantic Oscillation, surface current velocities, and SST changes in the subpolar north Atlantic. *J. Clim.* 16, 2355.
- Furevik, T., 2001. Variations of mixed layer properties in the Norwegian and Barents Seas: 1980–1996. *Deep-Sea Res.* 48, 383–404.
- Furevik, T., Mauritzen, C., Ingvaldsen, R., 2007. The flow of Atlantic Water to the Nordic Seas and Arctic ocean. In: Ørbaek, J.B., Kallenborn, R., Tombre, I., Hegseth, E.N., Falk-Petersen, S., Hoel, A.H. (Eds.), *Arctic Alpine Ecosystems and People in a Changing Environment*, vol. 2. Springer, Berlin, Heidelberg, pp. 123–146.
- Griffa, A., 1996. Applications of stochastic particle models to oceanographical problems. In: Adler, R., Muller, P., Rozovskii, B. (Eds.), *Stochastic Modelling in Physical Oceanography*. Birkhauser, pp. 114–140.
- Griffa, A., Owens, K., Piterberg, L., Rozovskii, B., 1995. Estimates of turbulence parameters from Lagrangian data using a stochastic particle model. *J. Mar. Res.* 53, 371–401.
- Helland-Hansen, B., Nansen, F., 1909. The Norwegian Sea. Its physical oceanography based upon the Norwegian researches 1900–1904. In *Report on Norwegian Fishery and marine investigations*, vol. II(1), Mallingske, Christiania, pp. 360.
- Holliday, N.P., 2008. Reversal of the 1960s to 1990s freshening trend in the northeast North Atlantic and Nordic seas. *Geophys. Res. Lett.* 35, L03614.
- Ingvaldsen, R., Asplin, L., Loeng, H., 2004. The seasonal cycle in the Atlantic transport to the Barents Sea during the years 1997–2001. *Cont. Shelf Res.* 24, 1015–1032.
- Isachsen, P., LaCasce, J.H., Mauritzen, C., Hakkinen, S., 2003. Wind-forced barotropic flow in sub-polar regions. *J. Phys. Ocean.* 33, 2534–2550.
- Isachsen, P., Mauritzen, C., Svendsen, H., 2007. Dense water formation in the Nordic Seas diagnosed from sea surface buoyancy fluxes. *Deep-Sea Res.* 54 (1), 22–41.
- Jakhelln, A., 1936. Oceanographic investigations in the East Greenland waters in the summers of 1930–1932. *Skrifter om Svalbard og Ishavet* 67, 76.
- Koszalka, I., LaCasce, J.H., Orvik, K.A., 2009. Relative dispersion in the Nordic Seas. *J. Mar. Res.* 67, 411–433.
- Koszalka, I., LaCasce, J.H., LaCasce, J.H., Andersson, M., Orvik, K.A., Mauritzen, C., 2011. Surface circulation in the Nordic Seas from clustered drifters. *Deep-Sea Res.* 58 (4), 468–485.
- LaCasce, J., 2005. Statistics of low frequency currents over the western Norwegian shelf and slope I: current meters. *Ocean Dyn.* 55, 213–221.
- LaCasce, J., 2008. Statistics from Lagrangian observations. *Prog. Oceanogr.* 77 (1), 1–29.
- LaCasce, J.H., 2000. Floats and f/H. *J. Mar. Res.* 58, 61–95.
- Lumpkin, R., Pazos, M., 2007. Measuring surface currents with SVP drifters: the instrument, its data, and some recent results. In: Griffa, A., Kirwan, A.D., Mariano, A.J., Ozgokmen, T., Rossby, T. (Eds.), *Lagrangian Analysis and Prediction of Coastal and Ocean Dynamics*. Cambridge University Press, pp. 39–67. (Chapter 2).
- Lumpkin, R., Maximenko, N., Pazos, M., 2012. Evaluating where and why drifters die. *J. Atmos. Oceanic Technol.*, 29, 300308. <<http://dx.doi.org/10.1175/JTECH-D-11-00100.1>>.
- Mauritzen, C., 1996. Production of dense overflow waters feeding the North Atlantic across the Greenland–Scotland Ridge. Part 1: evidence for a revised circulation scheme. *Deep-Sea Res.* 43, 769–806.
- Mork, K.A., Blindheim, J., 2000. Variations in the Atlantic inflow to the Nordic Seas, 1955–1996. *Deep-Sea Res.* 47, 1035–1057.
- Nilsen, J.E.Ø., Falck, E., 2006. Variations of mixed layer properties in the Norwegian Sea for the period 1948–1999. *Prog. Oceanogr.* 70, 58–90.
- Nøst, O.A., Isachsen, P.E., 2003. The large-scale time-mean ocean circulation in the Nordic Seas and Arctic Ocean estimated from simplified dynamics. *J. Mar. Res.* 61, 175–210.

- Orvik, K.A., Mork, M., 1996. Atlantic Water transports from long term current measurements in the Svinøy section. ICES CM 1996/O, 10 pp.
- Orvik, K.A., Skagseth, Ø., 2005. Heat flux variations in the eastern Norwegian Atlantic Current toward the Arctic from moored instruments, 1995–2005. *Geophys. Res. Lett.* 32, L14610.
- Orvik, K.A., Skagseth, Ø., Mork, M., 2001. Atlantic inflow into the Nordic Seas: current structure and volume fluxes from moored current meters, VM-ADCP and Sea-Soar-CTD observations, 1995–1999. *Deep-Sea Res. I* 48, 937–957.
- Polyakov, I.V., Beszczynska, A., Carmack, E.C., Dmitrenko, I.A., Fahrbach, E., Frolov, I.E., Gerdes, R., Hansen, E., Holfort, J., Ivanov, V.I., Johnson, M.A., Karcher, M., Kauker, F., Morison, J., Orvik, K.A., Schauer, U., Simmons, H.L., Skagseth, Ø., Sokolov, V.T., Steele, M., Timokhov, L.A., Walsh, D., Walsh, J.E., 2005. One more step toward a warmer Arctic. *Geophys. Res. Lett.* 32, L17605.
- Poulain, P.-M., Warn-Varnas, A., Niiler, P.P., 1996. Near-surface circulation of the Nordic Seas as measured by Lagrangian drifters. *J. Geophys. Res.* 101, 18237–18258.
- Press, W.H., Teukolsky, S.A., Vetterling, W.T., Flannery, B.P., 1992. *Numerical Recipes: The Art of Scientific Computing*, 2 ed. Cambridge University Press, Cambridge.
- Rodean, H.C., 1996. *Stochastic Lagrangian Models of Turbulent Diffusion*. American Meteorological Society, Boston, Massachusetts, US.
- Rossby, H.T., Riser, S.C., Mariano, A.J., 1983. The western North Atlantic—a Lagrangian viewpoint. In: Robinson, A.R. (Ed.), *Eddies in Marine Science*, Heidelberg, pp. 66–91.
- Rossby, T., 2007. Evolution of Lagrangian methods in oceanography. In: Griffa, A., Kirwan, A.D., Mariano, A.J., Ozgokmen, T., Rossby, T. (Eds.), *Lagrangian Analysis and Prediction of Coastal and Ocean Dynamics*. Cambridge University Press, pp. 1–38 (Chapter 1).
- Rossby, T., Ozhigin, V., Ivshin, V., Bacon, S., 2009. An isopycnal view of the Nordic Seas hydrography with focus on properties of the Lofoten Basin. *Deep-Sea Res. I* 56 (11), 1955–1971.
- Rudels, B., Jones, E.P., Schauer, U., Eriksson, P., 2004. Atlantic sources of the Arctic Ocean surface and halocline waters. *Polar Res.* 23 (2), 181–208.
- Saetre, R., 1999. Features of the central Norwegian shelf circulation. *Cont. Shelf Res.* 19, 1809–1831.
- Skagseth, Ø., 2008. Recirculation of Atlantic Water in the eastern Barents Sea. *Geophys. Res. Lett.* 35, L11606.
- Søiland, H., Prater, M.D., Rossby, T., 2008. Rigid topographic control of currents in the Nordic Seas. *Geophys. Res. Lett.* 35, L18607.
- Sundby, S., Drinkwater, K., 2007. On the mechanisms behind salinity anomaly signals of the northern North Atlantic. *Prog. Oceanogr.* 73, 190–202.
- Sutton, R.T., Allen, M.R., 1997. Decadal predictability of North Atlantic sea surface temperature and climate. *Lett. Nat.* 388, 563–567.
- Thompson, D.J., 1987. Criteria for the selection of stochastic models of particle trajectories in turbulent flows. *J. Fluid Mech.* 180, 529–556.
- Veneziani, M., Griffa, A., Reynolds, A.M., Mariano, A.J., 2004. Oceanic turbulence and stochastic models from subsurface Lagrangian data for the Northwest Atlantic Ocean. *J. Phys. Ocean.* 34, 1884–1906.
- Wadley, M.R., Bigg, G.R., 2006. Are great salinity anomalies advective? *Journal of Climate—Special Section* 19, 1080–1087.